# Hydroacoustic-elastic response of floating circular disk by FEM-BEM-EEM direct coupling method

## Ikjae Lee and Moohyun Kim

Department of Ocean Engineering, Texas A&M University, College Station, TX 77845, USA
ijlee@tamu.edu

## 1. INTRODUCTION

Fluid compressibility plays a crucial role in various ocean engineering problems. For instance, hydroacoustic waves generated by tsunamigenic sources due to the compressibility of water column gain attention by many researchers as tsunami precursor as a component of Tsunami Early Warning Systems [1]. That study also reported that fluid compressibility reduces phase speed of tsunami waves. In addition, so-called "seaquakes" are hydroacoustic waves produced by submarine earthquakes as a result of compressibility effect [2, 3]. Beyond these, numerous theoretical studies on hydro-acoustic waves have been conducted, e.g., [4]. More recently, an in-depth discussion of the "static compression" term and the derivation of governing equation were presented in Ref. [5].

On the other hand, the hybrid integral-equation method (HIEM) couples the boundary element method (BEM) for the interior domain with the eigenfunction expansion method (EEM) for the exterior domain, enabling the treatment of arbitrary seabed topography and floating-body geometry while naturally satisfying radiation condition [6]. An extension to the Helmholtz equation was introduced to account for seaquake loads on floating offshore wind turbines [3, 7].

In this study, the hydro-elastic analysis of floating structures using a direct coupling method between shell FEM and BEM (see Refs. [8-10]) is extended to incorporate fluid compressibility based on the HIEM. Accordingly, the coupling of three distinct methods is implemented for the hydroacoustic-elastic analysis of floating structures.
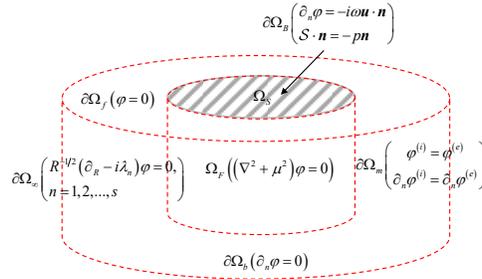
## 2. FORMULATION



Figure 1. Schematic of floating circular ice with boundary conditions: $\Omega_S$: structure domain; $\Omega_F$: fluid domain; $\partial\Omega_f$: free-surface; $\partial\Omega_B$: wetted body-surface; $\partial\Omega_b$: seabed boundary; $\partial\Omega_m$: matching-surface; $\partial\Omega_\infty$: boundary at infinity ($R \to \infty$). $\mu$ is wavenumber of acoustic wave, $\mathcal{S}$ is Cauchy stress tensor, and $p$ is fluid pressure. Spatial derivatives are defined by $\partial_n\varphi \equiv \boldsymbol{n}\cdot\nabla\varphi$ and $\partial_R\varphi \equiv \partial\varphi/\partial R$. The superscripts $(\bullet)^{(i)}$ and $(\bullet)^{(e)}$ denote interior and exterior domains, respectively.

In Figure 1, a schematic of floating ice with boundary conditions is given. The fluid and structure domains are coupled through interchange of kinematic and kinetic boundary conditions at body-surface $\partial\Omega_B$. The structure domain is described by finite element equilibrium equation, and the fluid domain is by potential flow satisfying Helmholtz equation as governing equation taking account of weak compressibility. The flow field is solved by HIEM by subdividing the entire fluid domain into interior and exterior sub-domains, and these are matched through two matching boundary conditions. In the HIEM, the interior domain is

solved by boundary element method (BEM), and the exterior domain is by eigenfunction expansion method (EEM).

The displacement-based finite element equilibrium equation is given by:

$$-\omega^2 \rho_s \int_{\Omega_s} \bar{\boldsymbol{u}} \cdot \boldsymbol{u} \, dV + \int_{\Omega_s} \mathcal{E}(\bar{\boldsymbol{u}}) : \mathbb{C} : \mathcal{E}(\boldsymbol{u}) \, dV + \rho_f g \int_{\partial \Omega_B} (\bar{\boldsymbol{u}} \cdot \boldsymbol{n}) u_3 \, dS + \rho_f g \int_{\partial \Omega_B} x_3 \bar{\boldsymbol{u}} \cdot \mathcal{Q}(\boldsymbol{u}) \cdot \boldsymbol{n} \, dS = \rho_f i \omega \int_{\partial \Omega_B} (\bar{\boldsymbol{u}} \cdot \boldsymbol{n}) \varphi \, dS \quad (1)$$

where $\omega$ is wave frequency, $g$ is gravitational acceleration, $\rho_s$ and $\rho_f$ are respectively structural and fluid densities, $\boldsymbol{u}$ and $\bar{\boldsymbol{u}}$ are respectively displacement and virtual displacement vectors, and $\boldsymbol{n}$ is normal vector directing outwards from fluid into structure. $2\mathcal{E}(\boldsymbol{u}) \equiv \nabla \boldsymbol{u} + (\nabla \boldsymbol{u})^T$ is linear strain tensor with displacement gradient $\nabla \boldsymbol{u} \equiv \partial u_i / \partial x_j \, \boldsymbol{e}_i \otimes \boldsymbol{e}_j$, $\mathbb{C}$ is constitutive tensor describing linear elastic material, and $\varphi$ is velocity potential in complex plane, i.e., $\phi(\boldsymbol{x},t) = \mathrm{Re}\{\varphi(\boldsymbol{x})e^{-i\omega t}\}$. The deformation of surface is described by $\mathcal{Q}(\boldsymbol{u}) \equiv \mathcal{I}(\nabla \cdot \boldsymbol{u}) - (\nabla \boldsymbol{u})^T$ with identity tensor $\mathcal{I} \equiv \delta_{ij} \boldsymbol{e}_i \otimes \boldsymbol{e}_j$, which comes from Nanson's formula: $\tilde{\boldsymbol{n}} d\tilde{S} = \det(\mathcal{F}) \mathcal{F}^{-T} \cdot \boldsymbol{n} dS \approx \boldsymbol{n} dS + \mathcal{Q}(\boldsymbol{u}) \cdot \boldsymbol{n} dS$ with deformation gradient $\mathcal{F} \equiv \mathcal{I} + \nabla \boldsymbol{u}$. In the rigid-body special case, the surface deformation tensor reduces to $2\mathcal{Q}(\boldsymbol{u}) = \nabla \boldsymbol{u} - (\nabla \boldsymbol{u})^T$. It should be noted that the floating ice is in equilibrium, thereby residual force and geometric stiffness terms are neglected. Also, MITC9 method was used to alleviate shear- and membrane-locking phenomena of thin shell structure [11].

On the other hand, a hybrid integral-equation is given by [6, 12]:

$$2\pi \begin{Bmatrix} \varphi^{(i)}(\boldsymbol{x}) \\ \varphi^{(e)}(\boldsymbol{x}) \end{Bmatrix} + \iint_{\partial \Omega_B} \varphi^{(i)}(\xi) \frac{\partial G}{\partial n'}(\boldsymbol{x};\boldsymbol{x}') dS + \iint_{\partial \Omega_m} \left\{ \varphi^{(e)}(\boldsymbol{x}') \frac{\partial G}{\partial n'}(\boldsymbol{x};\boldsymbol{x}') - G(\boldsymbol{x};\boldsymbol{x}') \frac{\partial \varphi^{(e)}}{\partial n'}(\boldsymbol{x}') \right\} dS \\ = -i\omega \iint_{\partial \Omega_B} G(\boldsymbol{x};\boldsymbol{x}') \boldsymbol{u} \cdot \boldsymbol{n}' dS \quad , \quad \forall \boldsymbol{x} \in \begin{cases} \partial \Omega_B \\ \partial \Omega_m \end{cases} \quad (2)$$

where $\boldsymbol{x}$ and $\boldsymbol{x}'$ are field and source points, and the Green's function $G(\boldsymbol{x};\boldsymbol{x}')$ is given by:

$$G(\boldsymbol{x};\boldsymbol{x}') = \frac{e^{i\mu r}}{r} + \frac{e^{i\mu r_2}}{r_2} \quad \text{with} \quad \begin{cases} r(\boldsymbol{x};\boldsymbol{x}') = \sqrt{(x-x')^2 + (y-y')^2 + (z-z')^2} \\ r_2(\boldsymbol{x};\boldsymbol{x}') = \sqrt{(x-x')^2 + (y-y')^2 + (z+z'+2h)^2} \end{cases}. \quad (3)$$

where acoustic wavenumber $\mu = \omega/c$ with acoustic wave speed in seawater $c = 1500 \, m/s^2$.

The velocity potential for exterior domain is represented by eigenfunction expansion as follows:

$$\varphi^{(e)}(\boldsymbol{x}) = \sum_{m=0}^{\infty} \sum_{n=1}^{\infty} f_n(z) \frac{Q_m(\lambda_n R)}{Q_m'(\lambda_n a)} (C_{mn} \cos m\theta + S_{mn} \sin m\theta), \quad \boldsymbol{x} \in \Omega_F^{(e)} (a \le R, -h \le z \le 0). \quad (4)$$

where $f_n(z) = \cos k_n(z+h)$ with $k_n h = (n-1/2)\pi$, $n = 1,2,...,\infty$, and

$$Q_m(\lambda_n R) = \begin{cases} H_m^{(1)}(\lambda_n R), & 1 \le n \le s \\ K_m(\lambda_n R), & s+1 \le n < \infty \end{cases} \quad \text{with} \quad \lambda_n = \begin{cases} \sqrt{\mu^2 - k_n^2}, & 1 \le n \le s \\ \sqrt{k_n^2 - \mu^2}, & s+1 \le n < \infty \end{cases}. \quad (5)$$

Here, $H_m^{(1)}$ is Hankel function of the first kind of order $m$, and $K_m$ is modified Bessel function of the second kind of order $m$. $s$ is maximum number of acoustic wave modes, and remaining stand for evanescent wave modes. The fluid resonance due to fluid compressibility occurs at $\mu = k_n$ ($\lambda_n \to 0$), which leads to infinitely large value in $Q_m(\lambda_n R)$. It can be observed that $k_n$ is determined by water depth, whereas $\mu (= \omega/c)$ is determined by wave frequency, i.e., the water depth significantly affects the resonance frequencies.

It should be noted that although gravitational waves are neglected in the exterior domain, the hydrostatic restoring is incorporated in the finite element equation, Eq. (1), i.e. flexural-acoustic-gravity waves are considered inside the interior domain.

## 3. COUPLED EQUATION

Iso-parametric map of displacement vector for shell FE model and velocity potential leads to a set of assembled discretized equations, and then FEM-BEM-EEM direct coupling yields a coupled algebraic equation of the form:

$$
\begin{bmatrix}
-\omega^2 M_{11} + K_{11} & -i\omega B_{12} & O \\
-i\omega B_{21} & K_{22} & K_{23} \\
-i\omega B_{31} & K_{32} & K_{33}
\end{bmatrix}
\begin{Bmatrix} \hat{u} \\ \hat{\varphi} \\ \hat{c} \end{Bmatrix}
=
\begin{Bmatrix} 0 \\ f_2 \\ f_3 \end{Bmatrix}
\tag{6}
$$

where finite-dimensional vectors, $\hat{u}$, $\hat{\varphi}$ and $\hat{c}$, stand for nodal displacement, nodal potential, and unknown coefficients for eigenfunctions, respectively. $f_2$ and $f_3$ stand for external hydroacoustic disturbances, not specifically given in Eq. (2), which might be either seismic or gravitational incident waves. Since the present study assumes inner-collocation-based high-order BEM that ensures uniform solid angle $2\pi$ over smooth surface. Otherwise, one needs to account for different solid angles of collocations points at vertices and edges. Accordingly, resulting matrix becomes over-determined system, and thus the method of least-square is employed. In this case, application of least-square method to total matrix leads to wrong output because of its approximation across different spaces $\hat{u} \in \mathcal{U}$, $\hat{\varphi} \in \mathcal{P}$, and $\hat{c} \in \mathcal{C}$. Accordingly, our strategy is to partition the total matrix into block matrices for each domain and then calculate condensed solutions.

## 4. RESULTS

### 4.1. Radiation of heaving disk

A floating disk is subjected to a forced heave motion. The water depth is $h = 5a$ with disk radius $a$. A rigid eigenvector for heave displacement $\hat{u} = \hat{\psi}_3$ is substituted into the coupled equation, which should be identical to applying heave boundary condition of rigid-body: $\partial_n \varphi = n_3$ on $\partial \Omega_B$. Figure 2 shows hydrodynamic pressure measured at center of the disk, this exhibits good agreement with the result given in Ref. [2], which verifies successful development of program. It should be noted that multiple peaks are due to the effect of fluid compressibility.
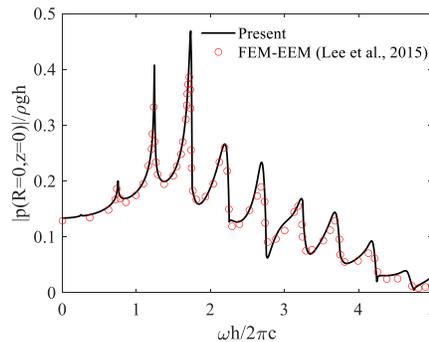


Figure 2. Hydrodynamic pressure at center of disk in forced heaving motion ( $h = 5a$ )

### 4.2. Hydroacoustic-elastic response by seismic incident waves

The seismic incident wave propagating from seabed to surface due to movement of flat seabed is given as a closed-form: $\phi_I(x,t) = \text{Re}\{\varphi_I(x)e^{-i\omega t}\}$ with $\varphi_I(x) = -\dfrac{i\omega\zeta}{\mu}\dfrac{\sin \mu z}{\cos \mu h}$, which satisfies harmonic seabed

motion $\partial_z \varphi_I = -i\omega\zeta$ at flat seabed $\partial\Omega_b$ (i.e., at $z = -h$) with $\zeta$ being amplitude of vertical ground motion. The modified hybrid integral-equation is given by:

$$2\pi \begin{Bmatrix} \varphi_D^{(i)}(\boldsymbol{x}) \\ \varphi_S^{(e)}(\boldsymbol{x}) \end{Bmatrix} + \iint_{\partial\Omega_B} \varphi_D^{(i)}(\boldsymbol{\xi}) \frac{\partial G}{\partial n'}(\boldsymbol{x};\boldsymbol{x}') dS + \iint_{\partial\Omega_m} \left\{ \varphi_S^{(e)}(\boldsymbol{x}') \frac{\partial G}{\partial n'}(\boldsymbol{x};\boldsymbol{x}') - G(\boldsymbol{x};\boldsymbol{x}') \frac{\partial \varphi_S^{(e)}}{\partial n'}(\boldsymbol{x}') \right\} dS$$
$$= -i\omega \iint_{\partial\Omega_B} G(\boldsymbol{x};\boldsymbol{x}') \boldsymbol{u} \cdot \boldsymbol{n}' dS + i\omega\zeta \iint_{\partial\Omega_b^{(i)}} G(\boldsymbol{x};\boldsymbol{x}') dS + \zeta \iint_{\partial\Omega_m} \varphi_I(\boldsymbol{x}') \frac{\partial G}{\partial n'}(\boldsymbol{x};\boldsymbol{x}') dS - 2\pi \begin{Bmatrix} 0 \\ \varphi_I(\boldsymbol{x}) \end{Bmatrix} \tag{7}$$

where $\varphi_D^{(e)} = \varphi_I + \varphi_S^{(e)}$ and two matching conditions, $\varphi_D^{(i)} = \varphi_D^{(e)}$ and $\partial_n \varphi_D^{(i)} = \partial_n \varphi_D^{(e)}$, were applied over $\partial\Omega_m$.

Based on Eq. (7), a study for rigid-body case (a floating offshore wind turbine subjected to seaquake loads) was successfully implemented by authors in Refs. [3, 7]. Results for flexible disks including sensitivity of water depth, which is closely linked to fluid resonance due to fluid compressibility, and dimension and material property of disk will be presented at the workshop site along with in-depth discussion.

## 5. CONCLUDING REMARKS

In this study, we developed a FEM-BEM-EEM direct coupling method. The proposed method is applicable to arbitrary geometry with curved surface, and locally variable seabed bathymetry inside the interior domain can be considered by manipulating image source of Green's function. Further, with minor modifications, acoustic-gravity waves can be considered for exterior domain, while the FE equilibrium equation already considers flexural-acoustic-gravity waves. More discussion on hydroacoustic-elastic response of a disk will be presented at the workshop site.

## REFERENCES

[1] Abdolali A, Kirby JT. Role of compressibility on tsunami propagation. Journal of Geophysical Research: Oceans. 2017;122:9780-94.
[2] Lee JH, Kim JK. Dynamic response analysis of a floating offshore structure subjected to the hydrodynamic pressures induced from seaquakes. Ocean Engineering. 2015;101:25-39.
[3] Lee I, Kim M, Kim H, Koo B. Earthquake and Seaquake Analysis for a 15MW Semi-Submersible Floating Offshore Wind Turbine (FOWT).  OCEANS 2024-Halifax: IEEE; 2024. p. 1-8.
[4] Zuccoli E, Kadri U. Resonant triad interactions of two acoustic modes and a gravity wave. Journal of Fluid Mechanics. 2025;1008:A15.
[5] Lu DQ, Yan XY. The governing equations for the hydro-acoustic waves in an inviscid compressible fluid with irrotational flows.  The 40th International Workshop on Water Waves and Floating Bodies. Shanghai, China2025.
[6] Yeung R. A hybrid integral-equation method for time-harmonic free-surface flow.  Proc 1st Int Conf on Num Ship Hydrod1975. p. 581-607.
[7] Lee I, Kim M. Seaquake loads by a hybrid integral equation method for dynamic analyses of floating offshore wind turbines under seabed earthquakes. Marine Structures (1st revision). 2026.
[8] Taylor RE. Hydroelastic analysis of plates and some approximations. Journal of engineering mathematics. 2007;58:267-78.
[9] Kim KT, Lee PS, Park K. A direct coupling method for 3D hydroelastic analysis of floating structures. International journal for numerical methods in engineering. 2013;96:842-66.
[10] Lee IJ, Kim ES, Kwon SH. A 3D direct coupling method for steady ship hydroelastic analysis. Journal of Fluids and Structures. 2020;94:102891.
[11] Bathe K-J, Lee P-S, Hiller J-F. Towards improving the MITC9 shell element. Computers & structures. 2003;81:477-89.
[12] Matsui T, Kato K, Shirai T. A hybrid integral equation method for diffraction and radiation of water waves by three-dimensional bodies. Computational mechanics. 1987;2:119-35.